PAPER • OPEN ACCESS

Efficient Removal of Pb(II) from Aqueous Solution using Zinc Oxide/Graphene Oxide Composite

To cite this article: S Z N Ahmad *et al* 2020 *IOP Conf. Ser.: Mater. Sci. Eng.* **736** 052002

View the article online for updates and enhancements.

Efficient Removal of Pb(II) from Aqueous Solution using Zinc Oxide/Graphene Oxide Composite

S Z N Ahmad,[1,2] **W N W Salleh,**[1,2] **N Yusof,**[1,2] **M Z M Yusop,**[1] **Hamdan, R,**[3] **N A Awang,**[1,2] **N H Ismail,**[1,2] **N Rosman,**[1,2] **H Ibrahim**[1] **and A F Ismail**[1,2]

[1]Advanced Membrane Technology Research Centre (AMTEC), Universiti Teknologi Malaysia, 81310 Skudai, Johor Bahru, Malaysia.
[2]School of Chemical and Energy Engineering, Faculty of Engineering, Universiti Teknologi Malaysia, 81310 Skudai, Johor Bahru, Malaysia.
[3]Faculty of Civil and Environmental Engineering, Universiti Tun Hussein Onn Malaysia, 86400 Parit Raja, Batu Pahat, Johor, Malaysia.

Corresponding author: hayati@petroleum.utm.my

Abstract. Due to the rapid development of industrialization over the years, the enhancement on heavy metals removal technology are becoming more urgent. Graphene oxide (GO) gained attention as adsorbents due to high surface area and high affinity towards heavy metals removal. However, its tendency for agglomeration and difficulty in phase separation urges more researches done to address its drawback. Zinc oxide (ZnO), a versatile nanomaterial, has been discovered to have high affinity towards heavy metals removal, tendency to spread out across GO sheet and ease of handling. Therefore, in this study, zinc oxide/graphene oxide nanocomposites (ZnO/GO) were synthesized as adsorbents for the removal of Pb(II) from aqueous solution. The synthesized composite was characterized using Fourier-transform Infrared Spectrometry (FT-IR), Scanning Electron Microscopy (SEM) and X-ray Diffraction (XRD), and had confirmed the chemically bonding of ZnO on GO. From the batch test, the optimum adsorbent dosage and initial pH for Pb(II) adsorption using ZnO/GO were 0.16 g/L and at pH 5, respectively, with the adsorption capacity of Pb(II) at 418.78 mg/g. The most rapid adsorption had occurred in the first 30 minutes, and the equilibrium time was achieved at 160 minutes. Also, Pb(II) adsorption had followed the pseudo-first order kinetic model. Therefore, ZnO/GO is thought to be a newly promising adsorbent in removing Pb(II) ion from the aqueous solution.

1. Introduction

To date, wastewater pollution due to the contamination of heavy metals has always been a global issue. Among the most common heavy metals found to be contaminating the water bodies are lead (Pb), cadmium (Cd), chromium (Cr), copper (Cu), zinc (Zn), and mercury (Hg). Pb(II) is a well-known toxic metal, of which it has an extensively wide application in the current industry, such as metal plating, lead-acid batteries, fuels, and radiation armor material [1]. Exposure of lead may cause various disorders on the human body systems, for instance, digestive, neurologic, cardiovascular, urinary, and respiratory-related diseases [2]. Therefore, it is critical for the industries, particularly and

generally all other lead-pollution sources, to enhance their wastewater treatment technology to prevent Pb(II) from entering the water bodies.

According to Malar [3], the pollution caused by metals need much more effort to be treated due to their rigid properties when involving biochemical reactions. Therefore, researchers have come out with a number of removal technologies with the aim to remove heavy metals from the aqueous solution, and some of these technologies have been extensively explored. Some of the methods are ion exchange, membrane filtration, chemical precipitation, and adsorption [4]. From the various methods utilized, adsorption method becomes one of the most popular processes in the removal and remediation of Pb. Adsorption is a promising choice due to its simple, low-cost and ease of operation, while being insensitive to toxic and harmful compounds [5].

The utilization of adsorbents, which is cost-effective and convenient in terms of operation and performances, is highly desirable and the pursuit of refining as well as discovering the most reliable adsorbents are still ongoing. Therefore, modification of highly promising adsorbents by functionalizing or grafting them with other potential adsorbents is becoming the focus of research on adsorbents nowadays. To mention a few, there are cellulose microspheres which are modified with magnetic chitosan [6], dextrin modified with poly m-phenylenediamine and graphene oxide [7], and ascorbic acid as carbon precursor enhanced with magnetic and mesosilicate-template [8].

Graphene oxide, a two-dimensional (2D) material, is advantageous to be used as adsorbents due to high surface-to-volume ratio and abundant oxygenated-functional groups (hydroxyl, carbonyl, carboxyl, and epoxy groups), whereby its hydrophilicity is enhanced in aqueous solution and it can serve as reactive sites for covalent bonding, dipole-dipole interaction or electrostatic interaction with the adsorbate [9]. Over the years, adsorbents developed from graphene-based materials have been extensively studied as heavy metals adsorbent due to their superior adsorption capability. Dialdehyde cellulose grafted graphene oxide [10], poly(ß-cyclodextrin)-magnetic graphene oxide [11], sulfonated graphene oxide [12], and 4-sulfophenylazo groups grafted on reduced graphene oxide [13] were a few examples of functionalized graphene-based materials explored for the purpose of removing heavy metals.

On the other hand, zinc oxide is a relatively cheap metal oxide that is widely used in the industries due to its excellent chemical and electrical properties. Besides that, zinc oxide nanoparticles has excellent porosity, which is an excellent property for effective and promising adsorbent. A few studies have been focusing on evaluating zinc oxide and zinc oxide-based materials as adsorbents, for instance, to remove Cu(II) [14], thiophene [15], and heavy metals [16]. By combining the excellent properties of both zinc oxide and graphene oxide, the zinc oxide/graphene oxide composite and their other ternary combinations have been studied on their performance as supercapacitor electrode [17], photocatalytic degradation of methylene blue [18], and adsorption of rhodamine B [19]. However, research on studying the performance of zinc oxide/graphene oxide composite as adsorbents to remove pollutants is still lacking.

Therefore, the present study focuses on the functionalization of zinc oxide (ZnO) on GO to synthesize zinc oxide/graphene oxide (ZnO/GO) composite for its performance in removing Pb(II) ion from synthetic wastewater solution. The adsorption capacity of this adsorbent is compared with GO on certain experimental conditions, such as initial pH effects, adsorbent dosage and contact time, while evaluating the affinity of both adsorbents towards the Pb uptake.

2. Materials and methods

2.1. Materials
Lead nitrate (Pb $(NO_3)_2$, graphite powder (<20 μm), $FeCl_2$, $FeCl_3$, and $NaNO_3$ were purchased from Sigma Aldrich. 30% H_2O_2, 25% ammonia solution, and acetone were bought from Merck. $Zn(CH_3COO)_2.2H_2O$ was from HmbG Chemicals, $KMnO_4$ from Bendosen, and H_2SO_4 and HCl were from R&M Chemicals. All chemicals were of analytical grade and used without further purification prior to analysis.

2.2. Preparation of GO

The synthesis of GO was done following the modified Hummers' method [20]. Initially, concentrated H_2SO_4 (69 mL) was cooled using ice bath to reach 0 ℃. After that, 3 g of graphite followed by 1.5 g $NaNO_3$ was dissolved into the cooled acid. The mixture was stirred for 15 minutes. Subsequently, $KMnO_4$ (9 g) was slowly added into the mixture; to prevent explosion, the temperature was maintained at below 20 ℃. After the mixture was stirred for 2 hours, the ice bath was replaced with water bath. Then, the temperature of the mixture was increased and maintained to 35 ℃, and then stirred for another half an hour. After that, RO water (500 mL) was added to the mixture followed by 30% H_2O_2 solution (15 mL) to terminate the reaction. The mixture was filtered and washed with 5% HCl solution until no sulfate was detected by $BaCl_2$. GO was later washed with RO water and kept inside the dialysis tubing membrane for a few days to neutralize the pH to 5–6. GO was then dispersed using ultrasonication for 2 hours prior to centrifugation at 10,000 rpm to separate the GO. Finally, the obtained GO was washed with acetone and dried in oven at 60 ℃ for 12 hours.

2.3. Preparation of ZnO/GO

The modification of GO using ZnO was done in the alkaline condition [21]. 2.97 g of $Zn(NO_3)_2.6H_2O$ was dissolved together with 0.1 g of the previously prepared GO in 100 mL of RO water and sonicated for 1 hour. Then, the mixture was cooled using an ice bath and the pH was adjusted to 8.3 using adequate amount of NaOH before being vigorously stirred for 20 minutes. Then, the product obtained was filtered, dried and heated in a furnace for 2 hours at 200 ℃.

2.4. Adsorbents characterization

The synthesized adsorbents, GO and ZnO/GO were characterized using Fourier-transform Infrared Spectrometer (FT-IR), Scanning Electron Microscopy (SEM), and X-ray Diffractometer (XRD). FT-IR was used to identify the functional groups present in the adsorbents and the instrument used was FT-IR Perkin Elmer spectrometer. The adsorbents were mixed with potassium bromide (KBr) and pressed into pellet prior to FT-IR analysis. SEM was utilized to discover the surface morphology of the fabricated adsorbents using Hitachi TM3000 Tabletop microscope. XRD analysis was done to identify the synthesized adsorbents, as well as assessing the degree of crystallinity of the sample. The instrument used was Rigaku Smartlab X-ray Diffractometer, and the analysis was done using Cu_K-beta filter at a scanning range of 3–100°.

2.5. Adsorption Batch Studies on the Removal of Pb(II)

The effects of initial pH solution, adsorbent dosage and contact time were investigated at atmospheric pressure and ambient temperature. In each glass bottle, 50 mL of 100 mg/L Pb(II) synthetic wastewater was prepared for batch test from colorless lead nitrate $(Pb(NO_3)_2)$ and the solvent used was RO water. To study the effects of initial pH, each Pb(II) solution was adjusted to pH 3–8 using adequate amount of NaOH and HCl before 10 mg adsorbent was added. The reaction was left to completion by shaking the reaction bottle on the platform shaker at 250 rpm for 24 h. For adsorbent dosage, 2, 4, 6, 8, 10, 12, and 14 mg of adsorbents were put inside each 50 mL of 100 mg/L Pb(II) solution and also shaken at 250 rpm for 24 h. For contact time study, 15 mL samples were taken at determined interval time until it reached 180 minutes. The analysis of Pb(II) ion concentration was done using flame atomic absorption spectroscopy (AAS). The samples were filtered using 0.45 m syringe filter prior to the AAS analysis.

3. Results and Discussion

3.1. Characterization of adsorbents

In order to determine the functional groups present in the adsorbents, analysis using Fourier-transform infrared spectroscopy (FT-IR) was performed. The peaks obtained for both GO and ZnO/GO are illustrated in Figure 1. For GO spectrum, the functional groups identified were of the same results, as

obtained by previous studies [20, 22]. Besides that, it can be seen that the incorporation of ZnO onto GO was achieved, with evidence from the combination of GO peaks in ZnO/GO as well as the presence of characteristic peak of ZnO bonding at 500.14 cm^{-1}. This high intensity peak confirmed the bonding vibration of Zn-O, which was also obtained by Sanmugam [23]. Meanwhile, at 3402.52 and 3414.97 cm^{-1} of GO and ZnO/GO spectra, these peaks indicated the presence of –OH stretching in the materials, which originated from the vibration of hydroxyl groups [24]. For GO spectrum, the peaks transmitted at 1716.70 and 1620.44 cm^{-1} pinpointed the presence of C-O stretching assigned for the vibration of carboxylic acid, while the latter signified the C=C stretching in the GO. For ZnO/GO, the stretching vibration for symmetrical C=O was found at 1572.51 cm^{-1}. There were vibrations of –OH deformation that had occured in both adsorbents, both of which were reflected at 1384.15 and 1407.43 cm^{-1} for GO and ZnO/GO, respectively. Besides that, peaks at 1113.89 cm^{-1} for GO and 1229.86 cm^{-1} for ZnO/GO were indicating the presence of C-O stretching in the alkoxy group. In addition, the vibrations that originated from the C-O stretching in the alkoxy group were represented via peaks at 1068 and 1022.05 cm^{-1} for GO and ZnO/GO, respectively. The –CH stretching peaks at 603.90 cm^{-1} and 677.41 cm^{-1} also confirmed that both of the adsorbents contained carbon compounds and the necessary oxygenated functional groups such as alkoxy, carboxyl and hydroxyl groups, all of which have high affinity in adsorbing Pb(II).
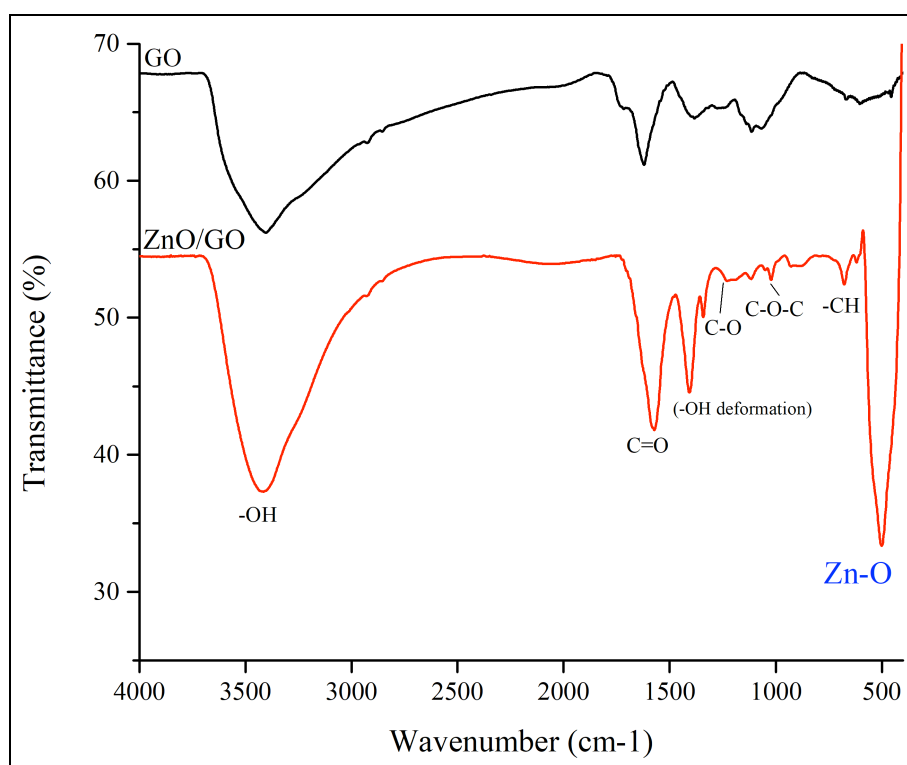
Figure 1. FT-IR spectra for GO and ZnO/GO.

For the analysis of surface morphology using Scanning Electron Microscopy (SEM), the morphology captured is shown in Figure 2. The image of GO appeared to be a material with irregular plane and little crumpled surfaces [25]. On the other hand, ZnO/GO showed the attachment of round-shape particles in abundance. These particles were stacked and agglomerated together, which covered almost 90% of the irregular GO sheet. These particles have further improved the porosities of the materials. The increase in porosity is thought to be advantageous for adsorbents due to its greater surface area for the adsorption of adsorbates [26].
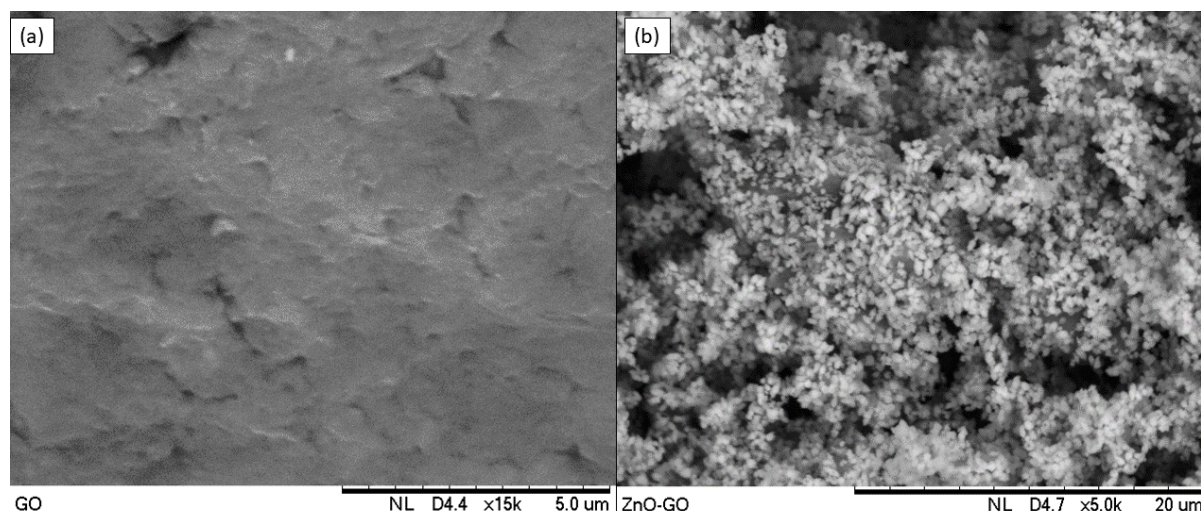
Figure 2. SEM image for (a) GO and (b) ZnO/GO.

Results from the X-ray Diffraction (XRD) analysis is shown in **Error! Reference source not found.**. The peak for GO was observed at $2\theta = 10.15°$ for (001) plane. The pattern of the lines also indicated that the GO was in an amorphous form. Undistinguished peaks were also observed, which might alarm the presence of unexfoliated graphite oxide and incomplete oxidation of graphite [27]. On the other hand, ZnO/GO showed matching identification peaks with zinc oxide (100), (101), (002), (102), (110), (103), (112), and (201) Bragg reflection plane. Apart from the characteristic peaks for ZnO, there was a presence of a tiny peak at $2\theta = 10.41°$ (001) plane of graphene oxide in the ZnO/GO XRD pattern. However, the intensity of the peak became very small. As suggested by Zhong & Yun [28], when ZnO particles intercalated in between the GO, it will cause the stacking of graphene oxide to be damaged, thus causing the peaks that resembled GO to be diminished. Consequently, this suggested that the incorporation of ZnO did not only occur at the top surface of the GO, but also in the surrounding area of the GO sheet.

3.2. Adsorption performance
To study the performance of the novel adsorbent ZnO/GO in the removal of Pb(II) from the aqueous solution, batch adsorption studies were conducted to compare the performance between GO and ZnO/GO. The influence of initial pH of the adsorbate, dosage of the adsorbent, and contact time between the adsorbent and adsorbate were investigated; the results obtained are illustrated in Figure 4. For the pH of the initial Pb(II) solution, at an acidic environment of pH 3, adsorbents showed the least Pb(II) adsorption capacity of 5.05 and 30.80 mg/g for GO and ZnO/GO, respectively. The protonation of carboxyl and hydroxyl groups at the surface of GO and ZnO/GO has caused an increase in the competition of adsorption site between the cations formed and divalent cation Pb(II). The adsorption of Pb(II) onto the surface of adsorbents were hindered when an abundant amount of cationic species repeled each other, since they are of the same charge. Besides that, when the carboxyl groups of GO were protonated, it caused GO to become less hydrophilic and tend to form aggregates [29]. Therefore, this caused a decrease in specific surface area for adsorption. Meanwhile, when the initial pH of the solution started to increase, GO showed a gradual increase in Pb(II) adsorption capacity up until pH 8. At a pH greater than 5, the pKa of carboxyl functional group was at 4.75; thus, the carboxyl functional group was deprotonated and became the negatively charged carboxylate ion that helped GO in adsorbing Pb(II) ion [30]. On the other hand, ZnO/GO showed a maximum increment for adsorption at pH 5, with an adsorption capacity of 427.21 mg/g. Then, the adsorption capacity started to decrease slightly, following the increase in pH. Therefore, the optimum pH for removal of Pb(II) from aqueous solution was pH 7 for GO at 214.75 mg/g, and pH 5 for ZnO/GO at 427.21 mg/g. The removal at pH 8

was not considered due to the precipitation of Pb(II) ion onto the lead hydroxide that had caused the removal of Pb instead of due to adsorption.
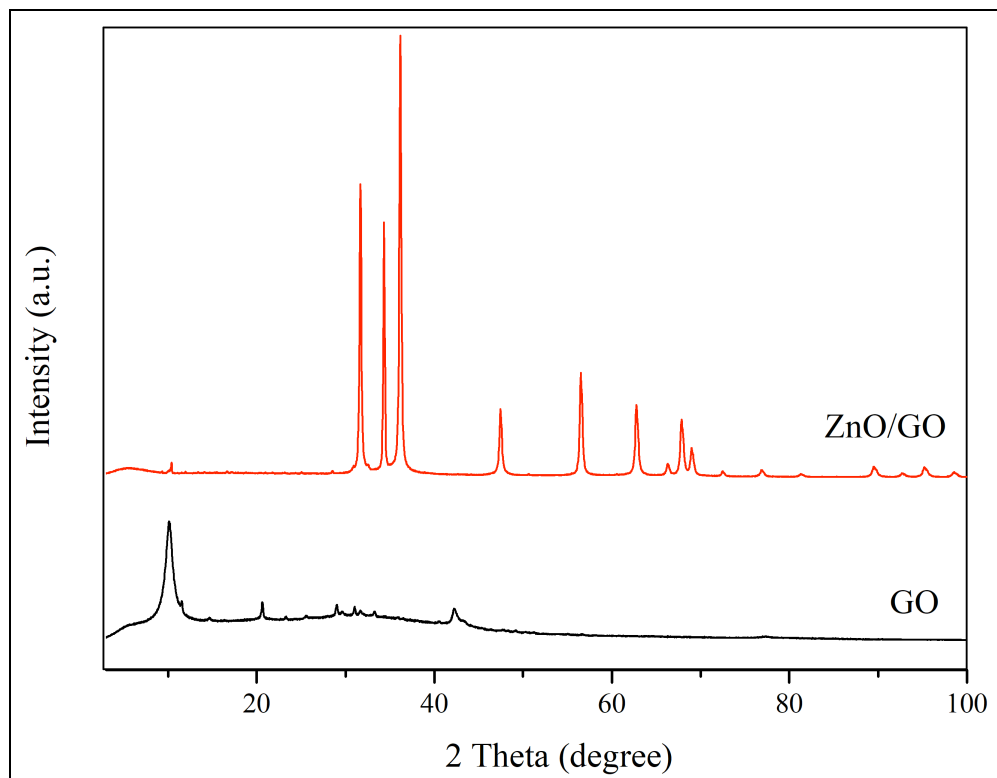
Figure 3. XRD pattern of GO and ZnO/GO.

From the investigation on adsorbent dosage, it could be seen from **Error! Reference source not found.**(b) that the optimum dosage of adsorbents needed was 10 mg for GO and 8 mg for ZnO/GO for the removal of 50 mL of 100 mg/L Pb(II). With that amount of adsorbents, the adsorption capacity obtained was 288.20 mg/g for GO and 418.78 mg/g for ZnO/GO. With the optimum adsorbent dosage (8 mg), the incorporation of ZnO on GO could increase the adsorption capacity to increase at 56.82% percentage increment, as compared to using its pure GO. Thus, the addition of ZnO was successful in increasing the adsorption capacity, as demonstrated by previous studies which incorporated ZnO with talc, graphene oxide and zeolite [31–33]. The adsorbent dosage needed was relatively lower for ZnO/GO as compared to GO, but the adsorption capacity of GO could increase drastically. After the optimum dosage, the adsorption capacity for GO remained consistent, while ZnO/GO showed a decrease in adsorption capacity when 10 mg and more of adsorbents were used. This suggested that the adsorbent dosage was in excess. With the same concentration of adsorbate, more adsorption sites have caused a random dispersed sorption, where the adsorption site occupied in a random distribution across the surface of the adsorbents and not only occupying certain adsorbents maximally.

Meanwhile, for the study of the effects of contact time on the adsorption capacity, the samples were collected at interval time until it reached 180 minutes. As shown in Figure 4(c), the first 10 minutes were the most rapid interval time for GO, while it took slightly longer for ZnO/GO for the most rapid adsorption period to be over with, which was in the period of 30 minutes. Initially, the entire specific adsorption site on the surface of adsorbent was unoccupied, thus, the initial adsorption capacity had increased abruptly. After some time, the amount of unoccupied or vacant site has been reduced since more sites are occupied; therefore, the gradient of the adsorption capacity began to increase more gradually as compared to before [34]. After the rapid period diminished, the adsorption capacity for ZnO/GO surpassed the adsorption capacity for GO. This showed the superiority of ZnO/GO as

compared to GO in the adsorption of Pb(II) from the aqueous solution. Eventually, the adsorption process reached equilibrium at 120 and 160 minutes with 211.96 and 227.46 mg/g for GO and ZnO/GO, respectively. Although ZnO/GO took a slightly longer time to achieve equilibrium relative to GO, the adsorption capacity of ZnO/GO is higher and the adsorbent dosage needed is lesser.
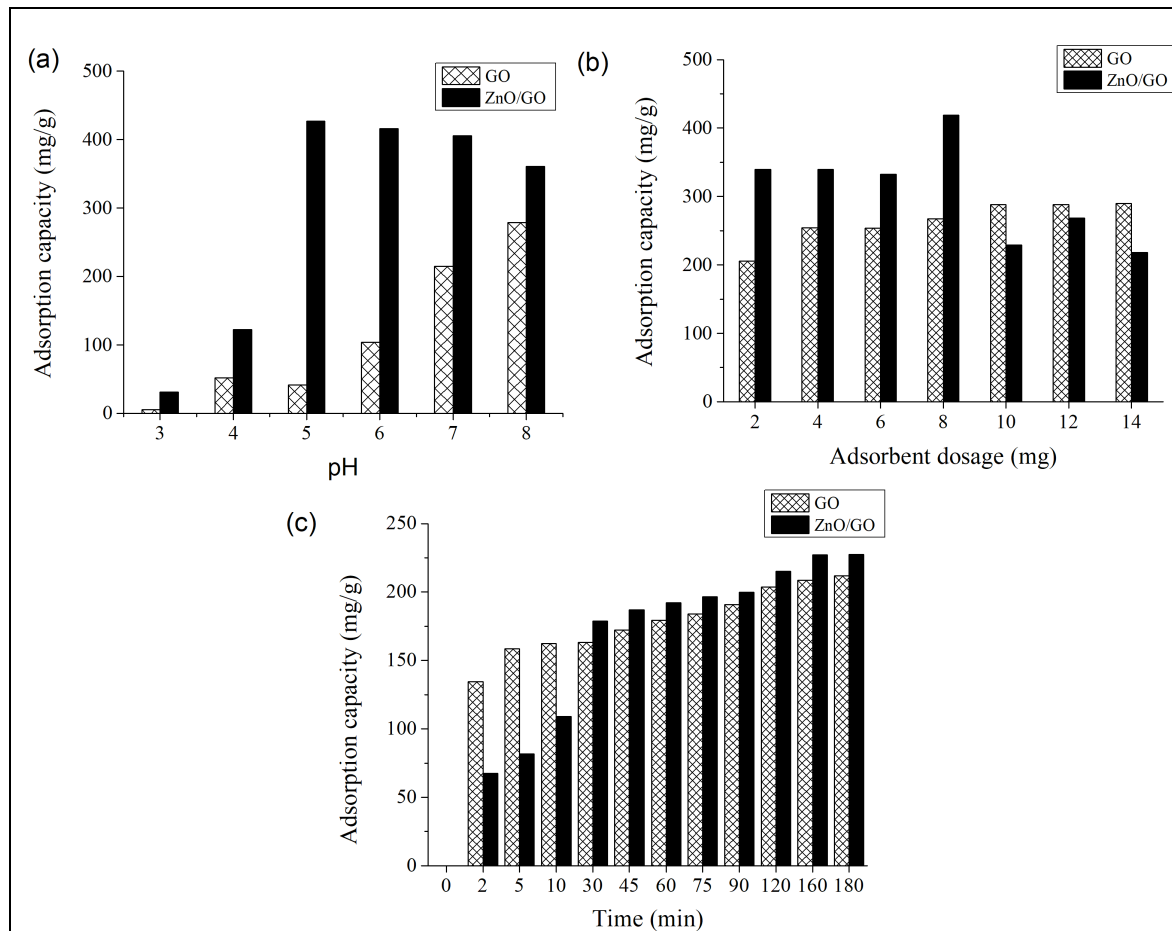
Figure 4. Pb(II) adsorption test for (a) pH effects (b) adsorbent dosage (c) contact time of GO and ZnO/GO.

3.3. Adsorption kinetics

To study the Pb(II) adsorption kinetics, the pseudo-first order and pseudo-second order kinetic models were analyzed. The equation for pseudo-first order were expressed by:

$$ln(q_e - q_t) = ln\,q_e - k_1\,t \qquad (1)$$

Meanwhile, for pseudo-second order, the equation is:

$$\frac{t}{q_t} = \frac{1}{k_2 q_e{}^2} + \frac{t}{q_e} \qquad (2)$$

where, q_e is the Pb(II) adsorption amount at equilibrium time (mg/g), q_t is the Pb(II) adsorption amount at designated time (mg/g), k_1 is the rate constant the pseudo-first order kinetic model, and k_2 is

the rate constant for the pseudo-second order kinetic model. The values k, q_e and correlation coefficient (R^2) of pseudo-first order and pseudo-second order kinetic models for both GO and ZnO/GO are tabulated in table 1. To obtain q_e and k_1 from the pseudo-first order, the graph of ln (q_e-q_t) against t was plotted; the value for q_e was obtained from the y-intercept and k_1 was obtained from the slope. For pseudo-second order kinetic, the values of q_e and k_2 can be obtained from the slope and intercept instead. From the R^2 calculated, it can be concluded that both Pb(II) adsorptions using GO and ZnO/GO as the adsorbents have followed the pseudo-first order; thus, the adsorption behavior occurred through physisorption [35]. Also, the calculated q_e when using pseudo-first order is similar to the experimental q_e than when using the pseudo-second order, which indicated the pseudo-second order kinetic model that pinpointed chemisorption as the mechanism was incapable of describing the adsorption of Pb(II) on the GO and ZnO/GO adsorbents [31].

Table 1. Pseudo-first order and pseudo-second order parameters.

Adsorbents	Pseudo-first order			Pseudo-second order		
	K_1 (min^{-1})	q_e	R^2	K_2 (gmg^{-1}min^{-1})	q_e	R^2
GO	0.35	229.02	0.9545	0.03	12.52	0.9584
ZnO/GO	0.27	279.58	0.9518	0.03	13.66	0.9450

4. Conclusion

The incorporation of ZnO into GO to synthesize the novel adsorbent has successfully increased 56.82% of the adsorption capacity, from 211.96 to 418.78 mg/g, of Pb(II) using ZnO/GO at an optimum dosage. The effects of the initial pH solution, adsorbent dosage and contact time have been studied. The optimum pH obtained was pH 5, while the optimum adsorbent dosage was 8 mg when removing 50 mL of 100 mg/L synthetic Pb(II) solution, or equivalent to 0.16 g/L. The equilibrium time was achieved at 160 min for ZnO/GO and the adsorption followed the pseudo-first order kinetic model. Thus, the new ZnO/GO adsorbent has high affinity towards the removal of Pb(II) from the aqueous solution, making it a promising adsorbent that can be further investigated for commercial use.

References

[1]   Zhang X, Lin Q, Luo S, Ruan K and Peng K 2018 *Appl. Surf. Sci.* **442** 322–31
[2]   Boskabady M, Marefati N, Farkhondeh T, Shakeri F and Farshbaf A 2018 *Environ. Int.* **120** 404–20
[3]   Malar S, Vikram S S, Favas P J C and Perumal V 2014 *Bot. Stud.* **55**(54) 1–11
[4]   Vilela D, Parmar J, Zeng Y and Zhao Y 2016 *Nano Lett.* **16**(4) 2860–6
[5]   Peng W, Li H, Liu Y and Song S 2017 *J. Mol. Liq.* **230** 496–504
[6]   Luo X, Zeng J, Liu S and Zhang L 2015 *Bioresour. Technol.* **194** 403–6
[7]   Zare E, Lakouraj M, and Kasirian N 2018 *Carbohydr. Polym.* **201** 539–48
[8]   Guo K, Larson S L and Ballard J H 2018 *Water, Air, & Soil Pollut.* **229**(122) 1–9
[9]   Pakulski D J, Czepa W, Witomska S, Aliprandi A, Pawluc P, Patroniak V, *et al.* 2018 *J. Mater. Chem. A* **20** 9384–90
[10] Yao A M, Wang Z, Liu Y, Yang G and Chen J 2019 *Carbohydr. Polym.* **212** 345–512
[11] Wang J, Zhang W, Wei J 2019 *J. Mater. Chem.* A **7**(5) 2055–65
[12] Wei M, Chai H, Cao Y, Jia D 2018 *J. Colloid Interface Sci.* **524** 297–305

[13]   Zhang C, Chen B, Bai Y, Xie J 2018 *Sep. Sci. Technol.* **53**(18) 2896–905
[14]   Rafiq Z, Nazir R, Raza M and Ali S. 2014 *Biochem. Pharmacol.* **2** 642–51
[15]   Singh S B and De M 2017 *J. Mater. Eng. Perform.* **27**(6) 2661–7
[16]   Khan S B, Rahman M M, Marwani H M, Asiri A M, and Alamry K A 2013 *Nanoscale Res. Lett.* **8** 1–8
[17]   Chee W K, Lim H N, Harrison I, Chong K F, Zainal Z, *et al.* 2015 *Ele.* **157** 88–94
[18]   Raghavan N, Thangavel S and Venugopal G 2015 *Mater. Sci. Semicond. Process* **30** 321–9
[19]   Wang J, Tsuzuki T, Tang B, Hou X, Sun L and Wang X 2012 *Appl. Mater. Interfaces* **4** 3084–90
[20]   Lai G S, Lau W J, Goh P S, Ismail AF, Yusof N and Tan Y H G 2016 *Desalination* **387** 14–24
[21]   Liu Y, Chen G, Tian C, Gupta R and Wang X 2018 *Environ. Technol.* **5** 1–9
[22]   Gong X, Liu Y, Wang Y, Xie Z, Dong Q, Dong M, *et al.* 2019 *Polymer* **168** 131–7
[23]   Sanmugam A, Vikraman D and Park H J 2017 *Nanomaterials* **7**(363) 1–14
[24]   Liu C, Qiu S, Du P, Zhao H and Wang L 2018 *Nanoscale* **10** 8115–24
[25]   Hao J, Ji L, Li C, Hu C and Wu K 2018 *J. Taiwan Inst. Chem. Eng.* **88** 137–45
[26]   Huang Y, Zeng X, Guo L, Lan J and Zhang L 2018 *Sep. Purif. Technol.* **194** 462–9
[27]   Drewniak S, Muzyka R, Stolarczyk A, Pustelny T, Kotyczka-Moranska M and Setkiwicz M 2016 *Sensors* **16**(103) 1-16
[28]   Zhong L and Yun K 2015 *Int. J. Nanomedicine* **10** 79–92
[29]   Shih C, Lin S, Sharma R, Strano M S and Blankschtein D 2012 *Langmuir* **28** 235–41
[30]   Ma Y, Lv L, Guo Y, Fu Y, Shao Q and Wu T, *et al.* 2017 *Polymer* **128** 12–23
[31]   Alswata A A, Bin M, Al-hada N M, Mohamed H, Zobir M, Hussein B, *et al.* 2017 *Results Phys.* **7** 723–31
[32]   Hosseini S A, Mashaykhi S and Babaei S 2016 *South African J. Chem.* **69** 105–12
[33]   Sani H A, Ahmad M B and Saleh T A 2016 *RSC Adv.* **6**(110) 108819–27
[34]   Pathania D, Sharma S and Singh P 2017 *Arab. J. Chem.* **10** 1445–51
[35]   Awang N A, Salleh W N W 2019 *J. Teknol.* **81**(2) 135–40